Journal of Biomechanics 118 (2021) 110293

Contents lists available at ScienceDirect

Journal of Biomechanics

journal homepage: www.elsevier.com/locate/jbiomech
www.JBiomech.com

Mixing and emptying of gastric contents in human-stomach: A numerical study

Changyong Li [a], Jie Xiao [b], Xiao Dong Chen [b], Yan Jin [a,*]

[a] Center of Applied Space Technology and Microgravity (ZARM), University of Bremen, Am Fallturm 2, 28359 Bremen, Germany
[b] Life Quality Engineering Interest Group, School of Chemical and Environmental Engineering, College of Chemistry, Chemical Engineering and Materials Science, Soochow University, Suzhou City, Jiangsu 215123, PR China

ARTICLE INFO

Article history:
Accepted 23 January 2021

Keywords:
Magenstrasse
Food boluses
Gastric motility
Food matrix
Computational fluid dynamics (CFD)

ABSTRACT

Stomach is one of the most important organs in human gastro-track. To better understand the operation of human-stomach, the process of mixing and emptying of gastric contents is simulated using a numerical method. The numerical results confirm that a fast pathway is located close to the lesser curvature of the stomach when water is emptied. However, this fast pathway doesn't exist when the gastric contents are composed of water and food boluses with different properties. The muscle contractions enhance the mixing of light food boluses and water, while they have limited effects on heavy food boluses. As a result, the foods are distributed in layers; heavy food boluses are located in the bottom layer. Besides the gastric motility and high viscosity of foods, the food matrix made of heavy food particles is also important to the formation of the Magenstrasse (stomach road). The food matrix and the zone of wrinkles behave like a porous medium which has higher flow resistance to the light food particles than to the water, leading to faster emptying of water. The water is emptied along the stomach wall since the flow resistance in the stomach wrinkles is smaller than the one in the food matrix. This mechanism is supported by the numerical results, while it might interpret the phenomena observed in the experiments.

1. Introduction

The stomach is a muscular, hollow organ in the upper digestive tract. The functions of stomach include releasing protein-digesting enzymes and hydrochloric acid (O'Connor and O'Moráin, 2014), mixing foods and gastric juice (Bornhorst et al., 2014), grinding large food particles (Kong and Singh, 2008), absorbing some small molecules (Hogben et al., 1957), etc. The obtained mixture, called chyme, is emptied by entering the duodenum through the pylorus under the control of the pyloric sphincter.

Mixing and emptying of gastric contents are the most important functions of stomach. The corresponding process is related to hydrodynamics, mass transfer, chemical reactions, etc. People believe the gastric motility of stomach plays an important role in this process. The gastric motility might help to grind the large food particles, enhance gastric mixing and thus affect the emptying rate (Bornhorst and Paul Singh, 2014; Ferrua and Singh, 2010; Miyagawa et al., 2016). Despite of these general knowledge, however, the mechanism for gastric mixing and emptying is still not fully understood due to its high complexity.

An important phenomenon related to gastric mixing and emptying is the Magenstrasse (stomach road), which describes the fast emptying of ingested liquids from the fed stomach (or postprandial stomach, denoting the stomach after eating, see (Grimm et al., 2017)). Based on a numerical study, (Pal et al., 2007) indicated that the antral contraction waves (ACWs) induce the Magenstrasse along a narrow and long pathway close to the lesser curvature of the stomach, which is the stomach region with shorter curvature (Podolsky et al., 2015). It might funnel liquid gastric contents from the farthest reaches of fundus directly to the intestine within 10 min. The *in vitro* experiments by (Chen et al., 2016) and (Wang et al., 2019) also confirmed that liquid gastric contents are emptied much faster than solid gastric contents.

The *in vivo* experiments by (Koziolek et al., 2016) and (Grimm et al., 2017) showed that the Magenstrasse plays an important role in the administration of drugs through the fed stomach. However, the long pathway close to the lesser curvature suggested by (Pal et al., 2007) was not found in the *in vivo* experiments. Instead, the water is found to flow around the chyme in the lumen along the entire stomach wall. The possible reason is that the gastric contents have a broad range of viscosity values. This observation is in

* Corresponding author.
E-mail address: yan.jin@zarm.uni-bremen.de (Y. Jin).

https://doi.org/10.1016/j.jbiomech.2021.110293
0021-9290/

accordance with the early experiment made by (Scheunert, 1912), who demonstrated that the water can flow around the gastric contents and thus reach the intestine faster. (Ferrua and Singh, 2015) also stated that, only water-like fluids are emptied in the long pathway close to the lesser curvature. This long pathway is even not found when tomato juice is emptied, although its properties are only mildly different from those of water. Therefore, the Magenstrasse is not a pure hydrodynamic problem, while the mixing of gastric contents with different properties should be investigated to understand its mechanism.

Mixing and emptying of gastric contents might be investigated using *in vivo* experiments, which are performed on living organisms or cells, or *in vitro* experiments, in which experiments are performed outside the biological body. However, due to the ethical problems and technical difficulties, it is hard to obtain all details of gastric mixing and emptying using *in vivo* or *in vitro* experiments. Compared with *in vivo* and *in vitro* experiments, numerical simulations may provide more details of gastric digestion. However, the current numerical simulations mainly focused on the fluid flows in stomach, see (Alokaily et al., 2019; Ferrua et al., 2014; Harrison et al., 2018; Ishida et al., 2019; Kozu et al., 2014; Pal et al., 2007) as examples. There is still a lack of studies regarding the mixing of gastric contents with different properties, despite of its significance in gastric digestion. In addition, very few numerical studies took all modes of muscle contractions of the stomach into account. To our knowledge, the tonic contraction (TC), which determines the gastric emptying rate, hasn't been simulated in previous numerical studies.

The purpose of this study is to better understand the mixing and emptying of gastric contents in human-stomach, particularly the physics of the Magenstrasse. To achieve this goal, the mixing and emptying process is simulated numerically. The mechanism for the Magenstrasse is studied based on the numerical results.

2. Mathematical model and numerical methods

A 3-dimensional human-stomach model is used in this study. It has similar characteristic length scales as real stomachs. Fig. 1 shows the stomach model schematically. The chemical reaction during the digestion process is neglected in this study, since it has only marginal effects on the Magenstrasse. The inlet of stomach (esophagus) is also neglected in the model because the esophagus sphincter is closed during the digestion process. Muscle contractions of the stomach are modeled by using dynamic mesh. They can be decomposed as tonic contraction (TC) and antral contraction (AC) (Indireshkumar et al., 2000). TC is a weak continuous contraction of stomach muscles which produces positive pressure differences between the stomach cavity and duodenum. AC consists of three phases: peristaltic contraction (PC), terminal antral contraction (TAC) and antral relaxation. PC is composed of ACWs, which initiate at the mid-corpus, and travel towards the terminal antrum. TAC is a segmental contraction of the terminal region of the antrum, which occurs when ACWs reach the terminal antrum (Schulze, 2006).

The gastric contents are supposed to be composed of water and food boluses in the early stage of digestion. Food boluses are a collection of solid food particles mixed with amylase-containing saliva (Kong and Singh, 2008). The statistical effects of the food particles on the continuous field can be accounted for by macroscopic properties, e.g., density, diffusion coefficient, and (apparent) viscosity. So N types of food boluses can be treated as fluids of N species. The mass fractions are $c_1, c_2, \ldots, c_N$, respectively. After food boluses are well mixed with water, the mixture is called chyme. The collection of small food particles suspended in the chyme can still be treated as a fluid, while large food particles usually deposit in the distal stomach, behaving like a porous matrix. This porous matrix hereby is called the food matrix, whereas it is different from the food matrix (micro-structure) discussed in (Kong and Singh, 2008), which has a much smaller length scale. The food matrix is relatively stable in the stomach due to the gastric sieving which prevents the large particles from passing through the pylorus.

We assume that the variation of food density is small. This assumption is in accordance with the density values in (Kozu et al., 2014; Xue et al., 2012). Thus, the gastric contents can be treated as an incompressible fluid, while the effect of density variation on momentum transport is accounted for by the Boussinesq approximation. The governing equations describe the conservation of the mass, momentum, and N food species, they read:

$$\rho_0 \frac{\partial u_i}{\partial x_i} = \dot{s}_g + \dot{s}_w \tag{1}$$

$$\frac{\partial u_i}{\partial t} + \frac{\partial (u_j u_i)}{\partial x_j} = -\frac{\partial p}{\partial x_i} + \frac{\partial \tau_{ji}}{\partial x_j} + \phi \frac{\rho_m - \rho_0}{\rho_0} g_i + \phi \dot{s}_{pi} \tag{2}$$

$$\frac{\partial c_n}{\partial t} + \frac{\partial (u_i c_n)}{\partial x_i} = \frac{\partial}{\partial x_i}\left(D_n \frac{\partial c_n}{\partial x_i}\right) + \dot{s}_{cn} \tag{3}$$

The stomach wrinkles and food matrix are modeled as porous medium zones with the porosity ϕ ($\phi = \phi_w$ in the winkles, $\phi = \phi_F$ in the food matrix). $\dot{s}_g$ and $\dot{s}_w$ in Eq. (1) are sources of mass due to the secretion of gastric juice and expansion/shrinking of wrinkles respectively. ρ_0 is the density of water, which is also used as the reference density.

ρ_m, g_i, and $\dot{s}_{pi}$ in Eq. (2) are the density of the mixture, gravity acceleration vector, drag force by the porous media, respectively. The Boussinesq approximation assumes gravity is strong sufficiently so the difference in inertia is negligible. The force due to the difference of density $\phi \frac{\rho_m - \rho_0}{\rho_0} g_i$ drives the heavy food boluses to sink and light food boluses to float. The density of the mixture is calculated as $\rho_m = \sum_{n=0}^{N} c_n \rho_n$. According to Darcy's law, $\dot{s}_{pi}$ is calculated as

$$\dot{s}_{pi} = \phi \frac{v_m}{K}(u_i - u_{si}) \tag{4}$$

The solid velocity u_{si} is approximated with the mesh cell velocity. $K = \frac{D_p^2 \phi^3}{180(1-\phi)^2}$ is the permeability calculated using the Carman–Kozeny equation (Nield and Bejan, 2006).

The source of mass due to expansion/shrinking of wrinkles introduces a source term $\dot{s}_{cn} = \dot{s}_w c_n / \rho_0$ in Eq. (3). D_n is the diffusion coefficient of the n^{th} species in the mixture. In order to investigate when the hydrogen ions (H^+) released together with the gastric juice reach the pylorus (the time scale of the Magenstrasse), the transportation equation of c_H (molar concentration of H^+) is solved, it reads

$$\frac{\partial c_H}{\partial t} + \frac{\partial (u_i c_H)}{\partial x_i} = \frac{\partial}{\partial x_i}\left(D_H \frac{\partial c_H}{\partial x_i}\right) + \dot{s}_{cH} \tag{5}$$

where D_H is the diffusion coefficient of H^+ in the mixture. $\dot{s}_{cH} = \dot{s}_g c_g / \rho_0 + \dot{s}_w c_H / \rho_0$ is the source term due to the secretion of gastric juice and expansion/shrinking of wrinkles. c_g is molar concentration of H^+ in the gastric juice.

Since the gastric contents are assumed to be incompressible, the mass of the gastric contents can be calculated as

$$G(t) = \int_\Omega \rho_0 \phi dV \tag{6}$$

In order to make the value of G identical to the objective function of mass $G_o(t)$, after the mesh is deformed, the porosity of the wrinkles ϕ_w is updated as

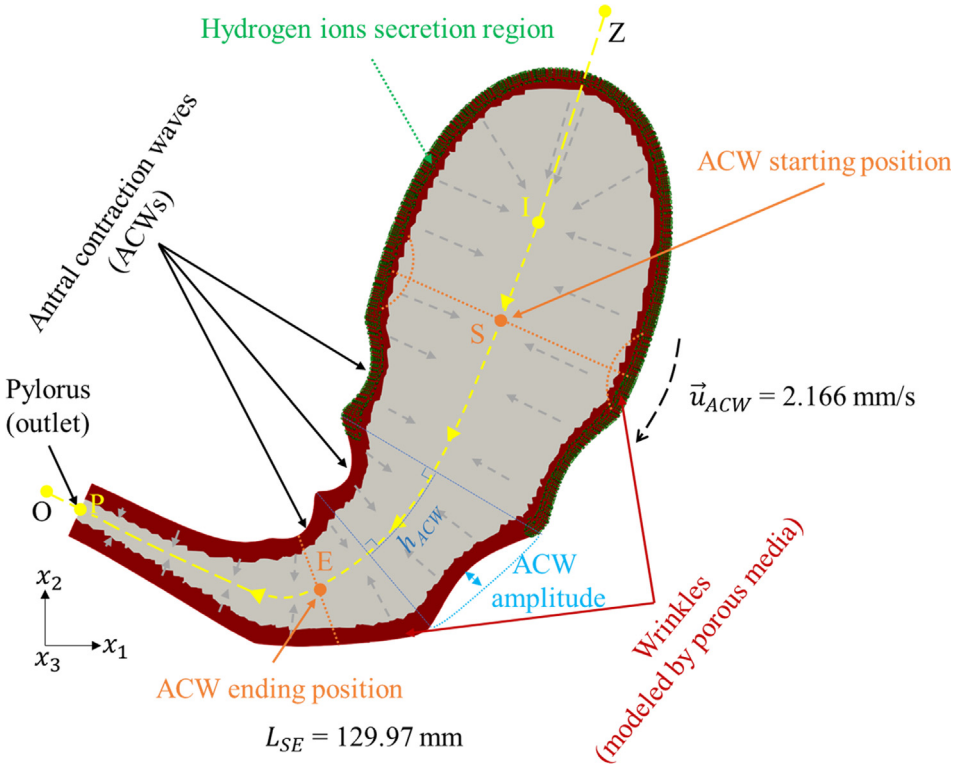

Fig. 1. The human-stomach model used in this study.

$$\phi_w = (G_o(t)/\rho_0 - V_t + V_w)/V_w \tag{7}$$

where V_t and V_w are the total stomach-volume and the volume of the wrinkles, respectively. Besides keeping the mass conservation, the variation of ϕ_w is also used to simulate the motility of wrinkles (expansion/shrinking).

The governing equations are solved using a finite volume method (FVM). The solver is developed based on the open source CFD program OpenFoam 18.06. A second-order implicit-backward scheme and a second-order central difference scheme are used for time and spatial discretization, respectively.

3. Description of test cases

The species properties used in this study are shown in Table 1. The properties of water and H^+ have the physical values. The properties of food boluses are given tentatively in this study but they are within the range of properties for the real foods. D_P of wrinkles is set to 1.6 mm (Huh et al., 2003) for calculation of the permeability K.

The test cases in this study can be classified as three groups, see Table 2. The emptying of water is studied in the test cases of group G1. Before the water-emptying process starts, the stomach is assumed to be filled with water. The initial velocity is 0. The initial H^+ concentration is 2.5×10^{-6} mol/L (pH ≈ 5.6) (Kong and Singh, 2008). Gastric juice is released in the porous medium zone (wrinkles) with the constant secretion rate (2.7×10^{-4} L/s) (Versantvoort et al., 2004) and H^+ concentration ($c_g = 2.5 \times 10^{-2}$ mol/L, pH ≈ 1.6) (Kong and Singh, 2008). For the water-emptying process, the muscle contraction is dominated by TC and PC (Ehrlein and Schemann, 2005). TAC doesn't occur in this process, while ACWs are released every 20 s (Harrison et al., 2018). The outlet (pylorus) is kept open during the water-emptying process.

The mixing of food boluses and water is studied in the cases of group G2. We set the outlet to be closed when the food-mixing process is simulated. The increase of mass due to secretion of gastric juice is neglected. Besides TC and PC, TAC plays also an important role during the food-mixing process, so it is accounted for in the simulation. TAC occurs every 20 s after 56 s, while it lasts for 4 s (King et al., 1984) each time (e.g. 56–60 s, 76–80 s, ...).

The emptying of the food and water mixture (chyme) is studied in the cases of group G3. The boundary and initial conditions in these cases are the same as those in group G2, except that the pylorus is kept open. The food matrix with ϕ_F = 0.4 and D_p = 0.4 mm (Villanueva-Carvajal et al., 2013) is considered in group G3.

Table 1
The properties of species in the study. ρ, D and ν are density, diffusion coefficient and kinematic viscosity, respectively.

Species	Color in Fig. 4	ρ [kg/m^3]	D [m^2/s]	ν [m^2/s]
Water	–	1000	–	1.0×10^{-6}
H^+	–	–	9.31×10^{-9}	–
FB1	Lavender	1000	6.6×10^{-9}	3.0×10^{-5}
FB2	Blue	1050	5.7×10^{-9}	7.0×10^{-5}
FB3	Green	1100	2.98×10^{-9}	9.0×10^{-5}
FB4	Red	1150	1.67×10^{-9}	1.0×10^{-4}
FB5	Black	1175	1.23×10^{-9}	2.0×10^{-4}

Table 2
Test cases in the study.

Group	Species	r_{emp} [kg/s]	Pylorus	Description
G1	Water, H^+	2.02×10^{-4}–8.51×10^{-4}	Open	Water-emptying
G2	Water, FB1-5	0	Closed	Water-food-mixing
G3	Water, FB1	2.02×10^{-4}	Open	Water-food-emptying

Two unstructured meshes are used in the study. They have about 6×10^5 cells (mesh A) and 2.3×10^6 cells (mesh B), respectively. According to the mesh-convergence study (shown below), mesh A is used in our analysis.

4. Results and discussion

We first studied the water-emptying process in the stomach. Fig. 2 shows the evolution of the pH-distribution with time. It might be observed that the H^+ close to the lesser curvature is more rapidly transported than the ones close to the greater curvature. The H^+ already reach the pylorus before 600 s. This phenomenon was also captured by (Pal et al., 2007) in their numerical study, which indicates that the Magenstrasse can funnel liquid gastric contents from the farthest reaches of fundus directly to the intestine within 10 min. As a result, more H^+ secreted at the lesser curvature of stomach will be brought out of the stomach. Fig. 3 shows the relationship between the volume averaged pH values ($\overline{\text{pH}}$) in the stomach and the mass of emptied gastric contents $G_{emp} = r_{emp} \cdot t$, where r_{emp} is the emptying rate. It can be seen that $\overline{\text{pH}}$ becomes slightly higher as a higher-resolution mesh is used, however, the numerical results are not qualitatively changed. So, mesh A is used in the study. Fig. 3 also shows that the gastric contents have a lower pH value as the emptying rate decreases.

However, the *in vivo* experiments by Koziolek et al. (2016) and Grimm et al. (2017) didn't show the exclusive Magenstrasse at the lesser curvature of stomach. The possible reason is that real food boluses have much more complicated properties than water. The mixing of food boluses and water is studied in the cases of group G2. Fig. 4a shows the initial distribution of food boluses, which are surrounded by water. Shortly after the mixing process starts (after a few seconds), the food mixture becomes multi-layered,

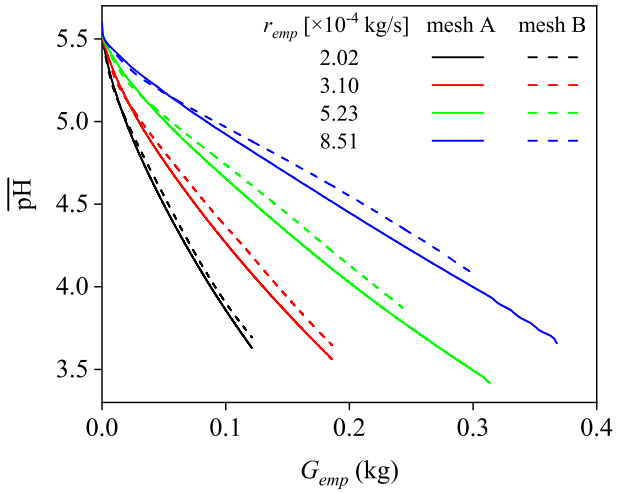

Fig. 3. Volume averaged pH value ($\overline{\text{pH}} = \frac{-\int_\Omega \log_{10}(c_H)dV}{\int_\Omega dV}$) in the stomach versus mass of emptied gastric contents G_{emp} for different emptying rates, G1.

see Fig. 4b. The heavy food boluses concentrate in the distal stomach. This is in accordance with the study by (Schulze, 2006), who stated that food is segmented in different layers inside the stomach. (Chen et al., 2016) also showed in their *in vitro* experiment that the food particles heavier than water fell down onto the greater curvature.

An important phenomenon with respect to food mixing is the "retropulsive jet-like motion", which is induced by the muscle contraction. Fig. 5 shows the vortical structures identified by the iso-surfaces of Q = 0.01 s^{-1} in a period of TAC, which starts at 56 s and ends at 60 s. The quantity Q is the second invariant of the

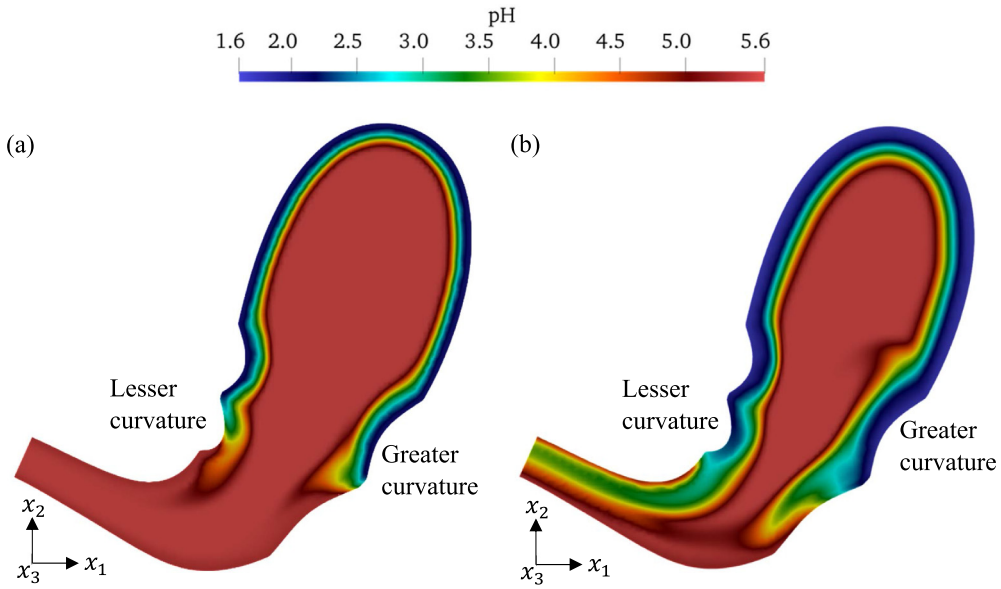

Fig. 2. Evolution of the pH-distribution in a cross section of the stomach. G1, r_{emp} = 2.02×10^{-4} kg/s. (a) t = 200 s, (b) t = 600 s.

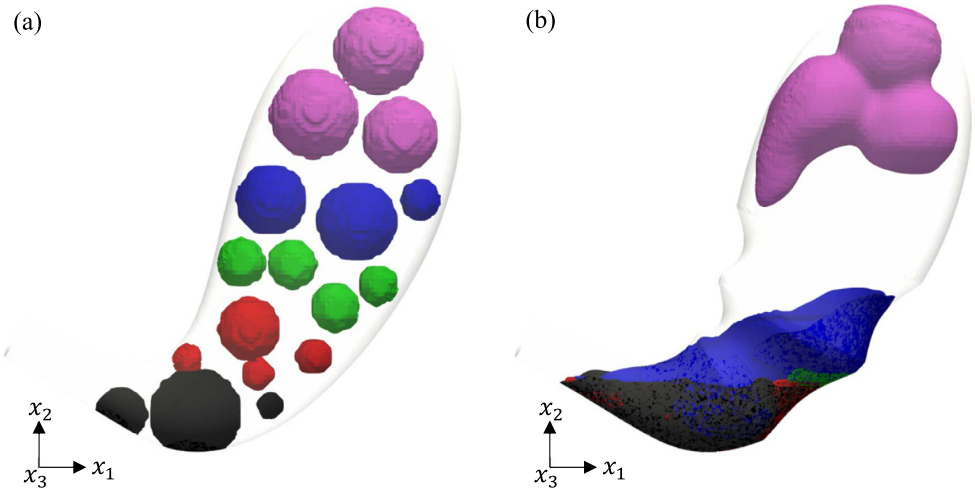

Fig. 4. Distribution of different food species in the stomach. The food species are shown in their colors indicated in Table 1 when their mass fraction $c_n \geq 0.1$, G2. (a) t = 0 s; (b) t = 600 s.

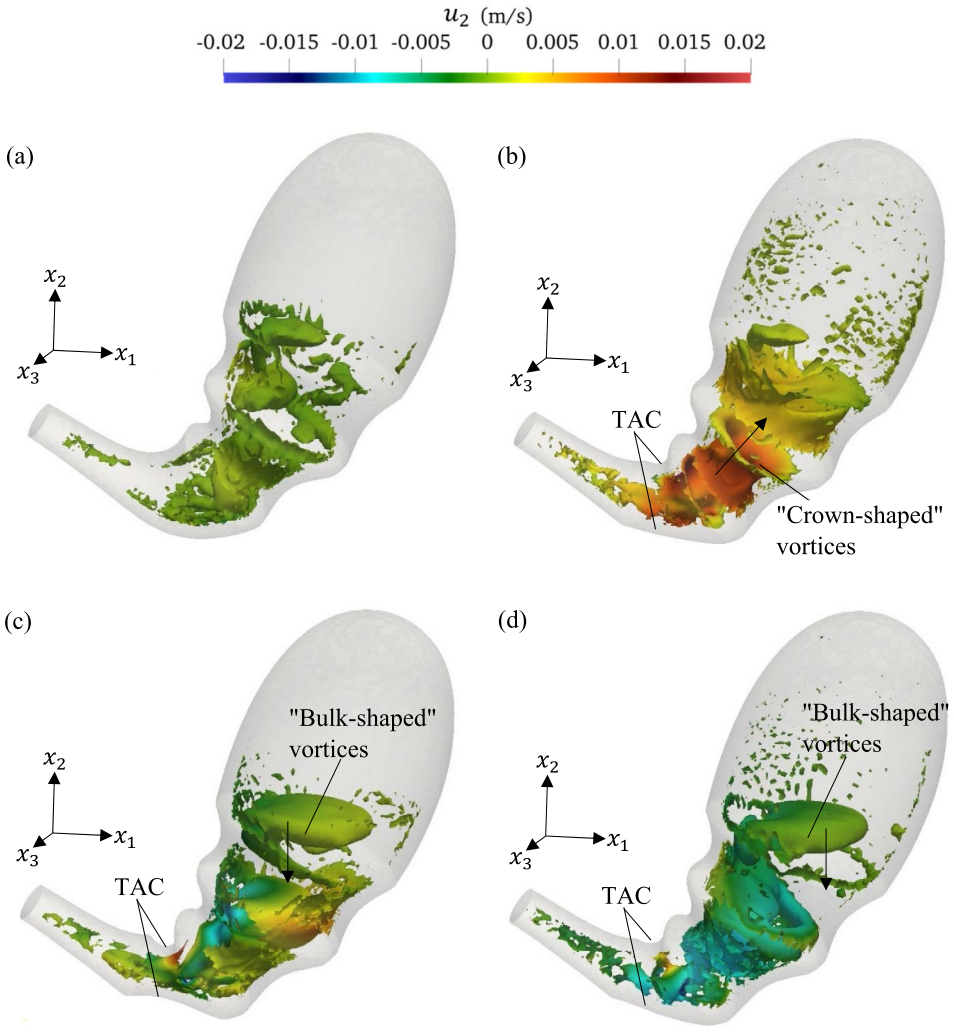

Fig. 5. Vortical structures identified by Q = 0.01 s^{-1} during a period of TAC, G2. The vortical structures are colored by the vertical velocity u_2. (a) t = 56 s; (b) t = 57 s; (c) t = 58 s; (d) t = 59 s.

instantaneous velocity gradient tensor for an incompressible flow (Hunt et al., 1988). The vortical structures are colored with the vertical velocity component (u_2) to indicate the direction of their motions. It can be seen that the food is forced back to the stomach by the TAC at 57 s. It sinks towards the terminal antrum at 59 s.

The similar "retropulsive jet-like motion" was also captured in the studies by (Ferrua et al., 2011; Ishida et al., 2019; Pal et al., 2004; Schulze, 2006). The transient flows are shown with velocity vectors in these studies. In our study, the coherent structures of the "retropulsive jet-like motion" are more clearly identified using the iso-surfaces of Q: Two shapes of large vortical structures are found in Fig. 5. "Crown-shaped" structures which have a high upward velocity can be observed when the gastric contents are ejected, see Fig. 5b. "Bulk-shaped" structures fall slowly when the TAC relaxes, see Fig. 5c. Besides the large vortical structures, we can also see small vortices close to the porous medium zone (modeled wrinkles). (Chen et al., 2016; Wang et al., 2019) stated that that the wrinkles help to grind the large food particles. The mechanism might be related to these vortices which result in the velocity variation in small length scales and thus the shear stress to cut the large food particles.

A mixing rate can be defined to quantify the extent of the food-mixing. For food species n, it is calculated as

$$r_{mix,n} = 1 - \frac{\int_\Omega \left(c_n - \bar{c}_n\right)^2 dV}{\int_\Omega \left(c_{n0} - \bar{c}_{n0}\right)^2 dV} \tag{8}$$

where $\bar{c}_n = \frac{1}{V}\int_\Omega c_n dV$ is the mean mass fraction of species n. c_{n0} and $\bar{c}_{n0}$ are the local and mean mass fraction of species n for the initial field, respectively. The mixing of a single food species and water is studied. Fig. 6a shows that the value of $r_{mix,n}$ increases monotonically with time when the food boluses have the same density as water (see the curve for FB1). The histories of $r_{mix,n}$ for food boluses FB2-5 are similar: The value of $r_{mix,n}$ increases to ~0.43 shortly after the mixing starts. Then, the value of $r_{mix,n}$ changes slowly due to the low efficiency of mixing. Fig. 6b shows the zoomed results during the period 300–360 s. A perturbation of $r_{mix,n}$ occurs during each TAC period, however, the TAC doesn't enhance the mixing of heavy foods.

In the test cases of food emptying (G3), the pylorus is kept open while the gastric contents are composed of water and food boluses FB1. The food boluses FB1 represent the small suspended solid particles which have the same density as water. Although the food boluses have higher viscosity than water, the water is not emptied faster than foods, see Fig. 7a. Therefore, gastric motility of stomach and high viscosity of foods are not sufficient for the formation of the Magenstrasse. Its mechanism needs to be more deeply investigated.

Our numerical results of food mixing (G2) show that the heavy food boluses will drop to the distal stomach shortly after ingestion, generating a food matrix. The flow resistance in the food matrix is determined by the Darcy's law. In the zone of food matrix as well as the zone of wrinkles, the flow resistance to the small food particles is much larger than the one to water, since the former has much higher viscosity. This may explain why small food particles are emptied more slowly than water.

It might be also noted that the length scale of large solid food particles is close to the length scale of stomach wrinkles. Thus, the region of wrinkles close to the stomach inner-surface cannot be perfectly filled with solid food particles. On the other hand, we expect that the food matrix has smaller permeability than the stomach wrinkles while food particles are stickier (resulting in higher viscosity). Therefore, the region close to the stomach inner-surface has lower flow-resistance than the food matrix. This may explain why (Koziolek et al., 2016) observed that the water ingested after a meal will flow around the chyme along the entire stomach wall.

Based on this understanding, we have calculated another test case in which a food matrix occupies part of the distal stomach. The porous matrix is assumed to move together with the dynamic mesh. Fast emptying of water doesn't occur when the food matrix is not considered (Fig. 7a). By contrast, the water is emptied faster than the food boluses due to the food matrix (Fig. 7b). The effect of the food matrix on the food mass fraction is shown in Fig. 8a and b, indicating that the food matrix slows down the transportation of the light food boluses to the pylorus. The effect of the food matrix on the velocity magnitude of water $c_0|\mathbf{u}|$ is shown in Fig. 8c and d. Due to the food matrix, the water flows close to the inner surface of stomach, leading to the Magenstrasse. The numerical results show that the motility of stomach, the high viscosity of food boluses, and the food matrix made of heavy food particles are the main reasons for the formation of the Magenstrasse.

5. Conclusion

The mixing and emptying of gastric contents in human stomach is investigated by using a CFD method to understand the mechanism of the Magenstrasse. Our numerical results confirm a fast pathway close to the lesser curvature of stomach for the H^+ to be transported to the pylorus when water is emptied, this is in accordance with the study by (Pal et al., 2007). However, this

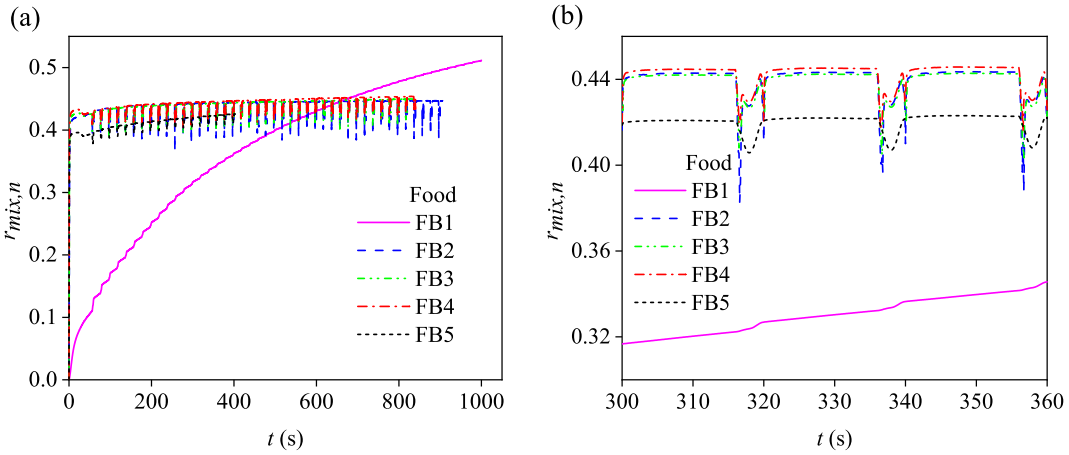

Fig. 6. The histories of $r_{mix,n}$ for the mixing of different food species with water, G2. (a) The results for the whole calculated period; (b) the results for the period 300–360 s.

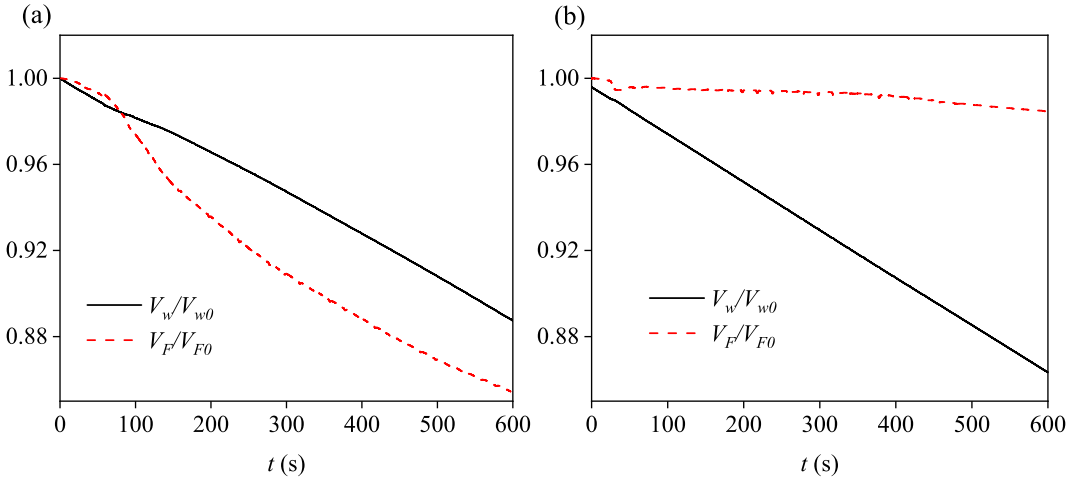

Fig. 7. Relative volumes of water V_w/V_{w0} and food boluses V_F/V_{F0} versus time, G3. (a) Without food matrix; (b) with food matrix.

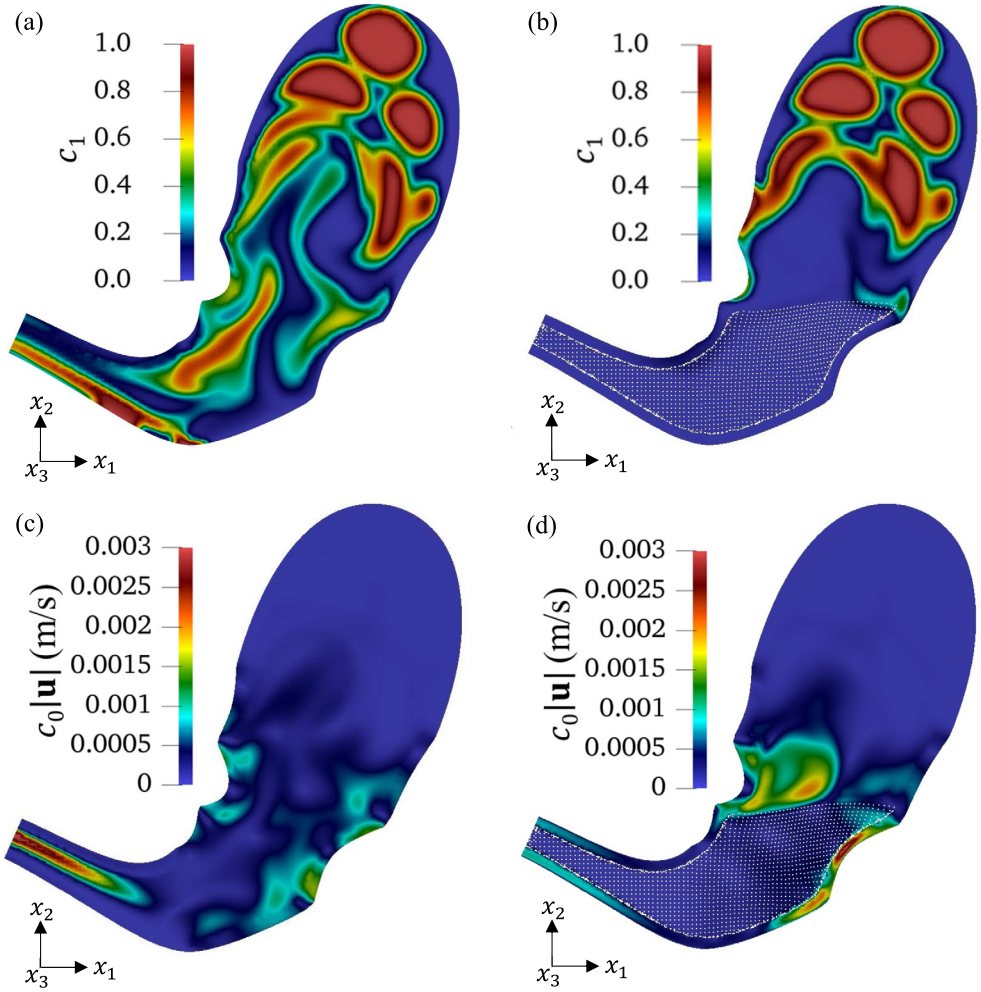

Fig. 8. Instantaneous food mass fraction and water-velocity fields in the stomach, G3, t = 250 s. (a) c_1, without food matrix; (b) c_1, with food matrix; (c) $c_0|\mathbf{u}|$, without food matrix; (d) $c_0|\mathbf{u}|$, with food matrix.

phenomenon doesn't occur when the gastric contents are made of food species with different properties.

When the gastric contents are mixed, TAC forces the gastric contents back into the proximal antrum, leading to the retropulsive jet-like motion. Two types of large vortices, "crown-shaped" and "bulk-shaped", are found in the central region of stomach during the retropulsive flow. Besides these large vortices, we have also found small vortical structures close to the wrinkles of stomach inner-surface. TAC enhances the mixing of water and light food boluses, however, it has limited effects on heavy food boluses,

leading to multi-layers of different food species. This phenomenon is consistent with the results of *in vivo* experiments, while it hasn't been captured in previous numerical studies.

Our numerical results support that the Magenstrasse is due to the gastric motility, high viscosity of food boluses, and the food matrix made of heavy food particles. The food matrix and stomach wrinkles have larger flow resistance to light food boluses (due to their higher viscosity) than to water. In addition, since the large solid food particles cannot perfectly fill the stomach wrinkles, the flow resistance close to the stomach inner-surface is lower than the one in the food matrix. As a result, the water is emptied rapidly close to the stomach inner-surface and around the chyme, leading to the Magenstrasse. The observation in previous *in vivo* experiments might be interpreted by this mechanism.

Declaration of Competing Interest

The authors declare that they have no known competing financial interests or personal relationships that could have appeared to influence the work reported in this paper.

Acknowledgement

We gratefully acknowledged the support of this study by China Scholarship Council (CSC) and the DFG-Heisenberg program (299562371).

Appendix A. Supplementary material

Supplementary data to this article can be found online at https://doi.org/10.1016/j.jbiomech.2021.110293.

References

Alokaily, S., Feigl, K., Tanner, F.X., 2019. Characterization of peristaltic flow during the mixing process in a model human stomach. Phys. Fluids 31, 103105.
Bornhorst, G.M., Paul Singh, R., 2014. Gastric digestion in vivo and in vitro: how the structural aspects of food influence the digestion process. Ann. Rev. Food Sci. Technol. 5, 111–132.
Bornhorst, G.M., Rutherfurd, S.M., Roman, M.J., Burri, B.J., Moughan, P.J., Singh, R.P., 2014. Gastric pH distribution and mixing of soft and rigid food particles in the stomach using a dual-marker technique. Food Biophys. 9, 292–300.
Chen, L., Xu, Y., Fan, T., Liao, Z., Wu, P., Wu, X., Chen, X.D., 2016. Gastric emptying and morphology of a 'near real'in vitro human stomach model (RD-IV-HSM). J. Food Eng. 183, 1–8.
Ehrlein, H., Schemann, M., 2005. Gastrointestinal Motility. Technische Universität München, Munich, pp. 1–26.
Ferrua, M., Singh, R.P., 2010. Modeling the fluid dynamics in a human stomach to gain insight of food digestion. J. Food Sci. 75, R151–R162.
Ferrua, M.J., Kong, F., Singh, R.P., 2011. Computational modeling of gastric digestion and the role of food material properties. Trends Food Sci. Technol. 22, 480–491.
Ferrua, M.J., Singh, R.P., 2015. Computational modelling of gastric digestion: current challenges and future directions. Curr. Opin. Food Sci. 4, 116–123.
Ferrua, M.J., Xue, Z., Singh, R.P., 2014. On the kinematics and efficiency of advective mixing during gastric digestion–A numerical analysis. J. Biomech. 47, 3664–3673.
Grimm, M., Scholz, E., Koziolek, M., Kühn, J.-P., Weitschies, W., 2017. Gastric water emptying under fed state clinical trial conditions is as fast as under fasted conditions. Mol. Pharm. 14, 4262–4271.
Harrison, S.M., Cleary, P.W., Sinnott, M.D., 2018. Investigating mixing and emptying for aqueous liquid content from the stomach using a coupled biomechanical-SPH model. Food Funct. 9, 3202–3219.
Hogben, C.A.M., Schanker, L.S., Tocco, D.J., Brodie, B.B., 1957. Absorption of drugs from the stomach. II. The human. J. Pharmacol. Exp. Ther. 120, 540–545.
Huh, C., Bhutani, M., Farfan, E., Bolch, W., 2003. Individual variations in mucosa and total wall thickness in the stomach and rectum assessed via endoscopic ultrasound. Physiol. Meas. 24, N15.
Hunt, J.C.R., Wray, A., Moin, P., 1988. Eddies, stream, and convergence zones in turbulent flows, Center for turbulence research report CTR-S88, pp. 193-208.
Indireshkumar, K., Brasseur, J.G., Faas, H., Hebbard, G.S., Kunz, P., Dent, J., Feinle, C., Li, M., Boesiger, P., Fried, M., 2000. Relative contributions of "pressure pump" and "peristaltic pump" to gastric emptying. Am. J. Physiol.: Gastrointest. Liver Physiol. 278, G604–G616.
Ishida, S., Miyagawa, T., O'Grady, G., Cheng, L.K., Imai, Y., 2019. Quantification of gastric emptying caused by impaired coordination of pyloric closure with antral contraction: a simulation study. J. R. Soc. Interface 16, 20190266.
King, P., Adam, R., Pryde, A., McDicken, W., Heading, R., 1984. Relationships of human antroduodenal motility and transpyloric fluid movement: non-invasive observations with real-time ultrasound. Gut 25, 1384–1391.
Kong, F., Singh, R.P., 2008. Disintegration of solid foods in human stomach. J. Food Sci. 73, R67–R80.
Koziolek, M., Grimm, M., Schneider, F., Jedamzik, P., Sager, M., Kühn, J.-P., Siegmund, W., Weitschies, W., 2016. Navigating the human gastrointestinal tract for oral drug delivery: uncharted waters and new frontiers. Adv. Drug Deliv. Rev. 101, 75–88.
Kozu, H., Kobayashi, I., Neves, M.A., Nakajima, M., Uemura, K., Sato, S., Ichikawa, S., 2014. PIV and CFD studies on analyzing intragastric flow phenomena induced by peristalsis using a human gastric flow simulator. Food Funct. 5, 1839–1847.
Miyagawa, T., Imai, Y., Ishida, S., Ishikawa, T., 2016. Relationship between gastric motility and liquid mixing in the stomach. Am. J. Physiol.-Gastrointestinal Liver Physiol. 311, G1114–G1121.
Nield, D.A., Bejan, A., 2006. Convection in Porous Media. Springer.
O'Connor, A., O'Moráin, C., 2014. Digestive function of the stomach. Dig. Dis. 32, 186–191.
Pal, A., Brasseur, J.G., Abrahamsson, B., 2007. A stomach road or "Magenstrasse" for gastric emptying. J. Biomech. 40, 1202–1210.
Pal, A., Indireshkumar, K., Schwizer, W., Abrahamsson, B., Fried, M., Brasseur, J.G., 2004. Gastric flow and mixing studied using computer simulation. Proc. R. Soc. Lond. Ser. B: Biol. Sci. 271, 2587–2594.
Podolsky, D.K., Camilleri, M., Fitz, J.G., Kalloo, A.N., Shanahan, F., Wang, T.C., 2015. Yamada's Textbook of Gastroenterology. John Wiley & Sons.
Scheunert, A., 1912. Über den Magenmechanismus des Hundes bei der Getränkaufnahme. Pflüger's Archiv für die gesamte Physiologie des Menschen und der Tiere 144, 569–576.
Schulze, K., 2006. Imaging and modelling of digestion in the stomach and the duodenum. Neurogastroenterol. Motil. 18, 172–183.
Versantvoort, C.H.M., Van de Kamp, E., Rompelberg, C.J.M., 2004. Development and applicability of an in vitro digestion model in assessing the bioaccessibility of contaminants from food. Report RIVM, Report 320102002/2004, Inspectorate of Health Inspection, Bilthoven.
Villanueva-Carvajal, A., Bernal-Martínez, L.R., García-Gasca, M.T., Dominguez-Lopez, A., 2013. In vitro gastrointestinal digestion of Hibiscus sabdariffa L.: The use of its natural matrix to improve the concentration of phenolic compounds in gut. LWT-Food Sci. Technol. 51, 260–265.
Wang, J., Wu, P., Liu, M., Liao, Z., Wang, Y., Dong, Z., Chen, X., 2019. An advanced near real dynamic in vitro human stomach system to study gastric digestion and emptying of beef stew and cooked rice. Food Funct. 10, 2914–2925.
Xue, Z., Ferrua, M.J., Singh, P., 2012. Computational fluid dynamics modeling of granular flow in human stomach. Alimentos hoy 21, 3–14.